Circular RNA PPP1CC promotes *Porphyromonas gingivalis*-lipopolysaccharide-induced pyroptosis of vascular smooth muscle cells by activating the HMGB1/TLR9/AIM2 pathway

Jie Liu[1], Yong Wang[1], Yaoyun Liao[1], Ying Zhou[1] and Jijin Zhu[2] ⓘ

Abstract

Objective: *Porphyromonas gingivalis* (*Pg*) plays a critical role in the occurrence and development of atherosclerosis. Lipopolysaccharide from *Pg* (*Pg*-LPS) could lead to pyroptosis of vascular smooth muscle cells (VSMCs) and induce instability of atherosclerotic plaque. Therefore, pyroptosis of VSMCs could promote the process of atherosclerosis. However, the exact mechanism of *Pg*-LPS-induced pyroptosis of VSMCs is unclear.

Methods: We determined pyroptosis and expression of interleukin (IL)-1β and IL-18 in VSMCs using 4′,6-diamidino-2-phenylindole staining and ELISA after stimulation by *Pg*-LPS. We established a knockdown plasmid containing the circular (circ)RNA PPP1CC and transfected it into VSMCs. Luciferase assays were performed to reveal the association between microRNAs miR-103a-3p and miR-107 and circRNA PPP1CC.

Results: Stimulation of *Pg*-LPS led to pyroptosis of VSMCs. Knockdown of circRNA PPP1CC relieved the *Pg*-LPS-induced pyroptosis of VSMCs and suppressed the expression of *HMGB1*, *TLR9*, *AIM2*, and cleaved caspase-1. Luciferase assays showed that PPP1CC directly targeted and competitively adsorbed miR-103a-3p and miR-107, weakening the inhibitory effect of these microRNAs on the expression of *HMGB1*.

[1]Health Care Department, Liuzhou People's Hospital, Liuzhou city, Guangxi Province, China
[2]Emergency Department, The First Affiliated Hospital of Guangxi Medical University, Nanning city, Guangxi Province, China

Corresponding author:
Jijin Zhu, Department of Emergency Medicine, The First Affiliated Hospital of Guangxi Medical University, No. 6, Shuangyong Road, Nanning city, Guangxi Province, 530021 China.
Email: Jijinzhu12@126.com

Conclusion: Knockdown of circRNA PPP1CC relieved *Pg*-LPS-induced pyroptosis of VSMCs. Pyroptosis of VSMCs appears to promote atherosclerosis and may represent a novel therapeutic target for its treatment.

Introduction

Atherosclerosis is a chronic disease of the circulatory system. The cardinal pathophysiological processes of atherosclerosis are leukocyte infiltration, inflammatory response of the blood vessels, and deposition of cell debris on the inner walls of the blood vessels.[1] Atherosclerosis is the primary cause of myocardial infarction and ischemic stroke, which are serious and life-threatening conditions.[2] Vascular smooth muscle cells (VSMCs) are the most common cell type in the arteries. During the occurrence and development of atherosclerosis, the proliferation of VSMCs is accelerated, resulting in vascular stenosis and fragility.[3,4] However, the apoptosis rate of VSMCs is also increased.[5,6] Subsequently, cell apoptosis gradually causes atherosclerotic plaque instability, increasing the risk of plaque rupture and detachment.[7–9] It has been reported that the expression level of caspase-3 is not significantly upregulated during the development of atherosclerosis, whereas that of caspase-1 is increased in atherosclerotic tissues.[10,11] Caspase-1 is a pyroptosis-related protein and its upregulation promotes secretion of interleukin (IL)-1β and IL-18.[12] Caspase-1 is also associated with plaque detachment.[13] These findings suggest that increased levels of proinflammatory cytokines induce cell pyroptosis, which in turn promotes the development of atherosclerosis.

Porphyromonas gingivalis (*Pg*) is a pathogen that contributes to dental plaque formation and the occurrence of periodontitis. It has been shown that *Pg*, which is present in atherosclerotic plaque, plays a crucial role in the occurrence and development of atherosclerosis.[14] In addition, a study revealed that periodontitis-induced systemic inflammation promoted vascular endothelial cell injury in mice and further aggravated atherosclerosis.[15]

The *AIM2* gene (absent in melanoma 2) may be activated by double-stranded DNA to form AIM2-ASC-procaspase-1 inflammatory corpuscle, thus promoting pyroptosis, a critical process in the maintenance of the body's innate immune system.[16] However, it has been reported that activation of the toll-like receptor 9 (TLR9)/myeloid differentiation primary response gene 88 (MyD88) pathway may also induce the expression of *AIM2* and high mobility group box 1B (*HMGB1*), which may be recognized by TLR9 receptors, thus enhancing the formation of AIM2-ASC-procaspase-1 inflammatory corpuscle by activating the TLR9/MyD88 pathway.[17]

Circular RNAs (circRNAs), a specific type of non-coding RNAs, are highly stable because of their ring structure.[18]

CircRNAs are present in many tissues and play a critical role in regulating diverse physiological processes of the human body.[19] Furthermore, circRNAs are thought to act as competitive RNAs that adsorb intracellular microRNAs (miRNAs), thereby attenuating the effect of miRNAs on the expression of the miRNAs' target proteins.[20] Screening results obtained from the competing endogenous (ce)RNA network predict that circular RNA serine/threonine-protein phosphatase PP1-gamma catalytic subunit (circPPP1CC) regulates the expression of *HMGB1* via 49 different miRNAs. However, whether circPPP1CC can promote atherosclerosis by affecting *Pg*-induced pyroptosis of human umbilical vein endothelial cells (HUVECs) via the HMGB1/TLR9/AIM2 pathway remains unclear.

In a recent study, lipopolysaccharide from *Pg* (*Pg*-LPS) was shown to affect the proliferation and adhesion of VSMCs and induce pyroptosis.[21] Therefore, we detected the effect of circPPP1CC on the Pg-LPS-induced pyroptosis and inflammation of vascular smooth muscle cells in this study. Furthermore, we clarified the molecular mechanism of this efficacy. The mechanism could provide a new therapeutic option for the clinical treatment of atherosclerosis.

Materials and methods

Ethics statement

This research was checked and approved by the ethics review committee of Liuzhou People's hospital.

Cell culture and treatment

HUVECs were obtained from the American Type Culture Collection (ATCC, Manassas, VA, USA) and cultured in RPMI-1640 medium (HyClone/GE Healthcare Life Sciences, Logan, UT, USA) supplemented with 10% fetal bovine serum (Gibco/Thermo Fisher Scientific Inc., Waltham, MA, USA) at 37°C in a humidified atmosphere of 5% CO_2. Small interfering (si) RNA targeting circPPP1CC was purchased from Shanghai GeneChem Co. Ltd. (Shanghai, China) and transfected into HUVECs using Lipofectamine 2000 (Invitrogen/Thermo Fisher Scientific Inc.). The mimic sequences of miR-103a-3p (mimic: 5′-TCATAGCCCTGTACAATGCTGCT-3′, negative control (NC): 5′-AUAGCCCUGUACAAUGCUGCUUU-3′) and miR-107 (mimic: 5′-GTACCGCCCGCCTTGATGCCGAA-3′, NC: 5′-AGCAGCAUUGUACAGGGCUAUGA-3′) were also obtained from Shanghai GeneChem Co. Ltd. Next, the mimic sequences (50 nmol/L) were transfected into the HUVECs, and Lipofectamine 2000 was used to promote the efficacy of transfection. These cells were used in subsequent experiments after 48 hours of transfection. All procedures were performed according to the manufacturer's instructions. HUVECs were cultured with different concentrations (10^{-3}, 10^{-4}, 10^{-5}, and 10^{-6} mol/L) of *Pg*-LPS (Sigma Aldrich/Merck KGaA, Darmstadt, Germany) for three to four generations to establish an in vitro model of pyroptosis.

Cell Counting Kit−8 assay

HUVECs were plated in 96-well plates. Following adhesion, cells were stimulated by *Pg*-LPS for 12, 24, and 48 hours, and then the Cell Counting Kit CCK-8 reagent (Dojindo Molecular Technologies Inc., Rockville, MD) was added into each well. Cells were incubated for an additional 1.5 hours, and the absorbance of each well was determined using a spectrophotometer.

Pyroptosis detection

Pyroptosis of HUVECs was determined by 4′,6-diamidino-2-phenylindole (DAPI) staining. Briefly, cells were seeded onto sterile glass coverslips, fixed with 4% paraformaldehyde, and permeabilized with 0.5% Triton X-100 (Beyotime Institute of Biotechnology, Shanghai, China). Subsequently, cells were rinsed with PBS 3 times and stained with DAPI staining solution. Cell nuclei were observed under a fluorescent microscope (Olympus Corp., Tokyo, Japan).

Luciferase assay

The materials and commercial kit were obtained from Promega Corp. (Madison, WI, USA). Luciferase assays were performed according to the manufacturer's instructions. Fluorescence was measured with a spectrophotometer (Thermo Fisher Scientific Inc.).

ELISA

The supernatants from cultured HUVECs were collected, centrifuged at $15,000 \times g$ and 4°C for 10 minutes, and transferred into sterilized tubes. Subsequently, a human IL-1β ELISA kit (cat. no. RAB0273; Sigma Aldrich/Merck KGaA), human IL-18 ELISA kit (cat. no. ab215539; Abcam, Cambridge, UK), and an HMGB1 antibody kit (cat. no. ab18256; Abcam) were used to detect secretion of IL-1β, IL-18, and HMGB1, respectively. All assays were performed according to the manufacturers' instructions.

Western blot analysis

Total proteins were extracted from HUVECs using radioimmunoprecipitation assay (RIPA) buffer (Beyotime Institute of Biotechnology). The concentration of the protein samples was measured with the bicinchoninic acid method (Beyotime Institute of Biotechnology). Subsequently, proteins were separated on a 10% sodium dodecyl sulfate-PAGE gel (Beyotime Institute of Biotechnology) and electrotransferred onto polyvinylidene fluoride (PVDF) membranes (EMD Millipore, Burlington, MA, USA). Following transfer, the PVDF membranes were blocked with 5% skim milk powder for 1.5 hours and incubated with primary antibodies at 4°C overnight. The primary antibodies were as follows: anti-cleaved caspase-1 (cat. no. 89332S), anti-HMGB1 (cat. no. 6893S), anti-TLR9 (cat. no. 13674S), anti-AIM2 (cat. no. 12948S), and anti-GAPDH (cat. no. 5174S; all from CST Biological Reagents Co. Ltd., Danvers, MA, USA). On the next day, the membranes were rinsed with PBS-Tween three times and incubated with a corresponding secondary antibody for 1.5 hours. The membranes were washed again with PBS-Tween and antibody reactivity was visualized using the Pierce Western Blotting Substrate (Thermo Fisher Scientific Inc.).

Reverse transcription–PCR

Total RNA was isolated with Trizol method (Invitrogen/Thermo Fisher Scientific Inc.) and reverse transcribed into cDNA using a reverse transcription kit (Takara Bio Inc., Shiga, Japan). Subsequently, the synthesized cDNA was used as the template for PCR amplification and the results were analyzed using the $2^{-\Delta\Delta Cq}$ method. All assays were performed according to the manufacturer's recommendations. The expression levels of miR-103a-3p and miR-107 were determined with the MicroRNA kit (Guangzhou Ribobio Co. Ltd., Guangzhou, China), and the results were normalized to U6 expression. The expression of circPPP1CC was normalized to expression of *GAPDH*. The primer sets for circPPP1CC, miR-103a-3p, and miR-107 were as follows:

circPPP1CC: forward 5′-CAGGAGAACTG TTGATGGCATA-3′, reverse 5′-ATACCC CTTGGAGGCGT TAC-3′; miR-103a-3p: forward 5′-ATCCA GTGCGTGTCGTG-3′, reverse 5′-TGCT AGCAGCATTGTA CAGG-3′; miR-107: forward 5′-TGTGT AGTAGTTTGTTTAT AGTG-3′, reverse 5′-CCAACTCTACAACTACTAAATC-3′; *GAPDH* forward 5′-GAAGGTGAAGGTC GGAGTC-3′, reverse 5′-GAAGATGGT GATGGGATTTC-3′.

Statistical analysis

All data were analyzed using GraphPad prism 6.0 software (GraphPad Software Inc., San Diego, CA, USA) and were presented as the mean ± standard deviation (SD). All experiments were repeated three times. Data in Figure 1 were analyzed using two-way ANOVA. Data were confirmed using the Tukey test. Multiple groups in Figure 2, Figure 3, and Figure 5 were compared by one-way analysis of variance (ANOVA) followed by the Scheffé post hoc test. Student's *t*-test was used to determine the significance between two groups,

and $P < 0.05$ was considered to indicate a statistically significant difference.

Results

Pg-LPS stimulation promoted proliferation of VSMCs

A study has shown that *Pg* may induce apoptosis and endoplasmic reticulum stress in HUVECs.[22] Therefore, we detected the proliferation rate of HUVECs using the CCK-8 assay. The results (Figure 1) showed that increasing concentrations of *Pg*-LPS gradually accelerated proliferation of HUVECs.

Pg-LPS stimulation enhanced pyroptosis of HUVECs

Pyroptosis of HUVECs was observed following staining of cell nuclei with DAPI. As shown in Figure 2a, cell nuclei swelled gradually and showed signs of rupture after stimulation with *Pg*-LPS. Given the critical role of caspase-1 in pyroptosis, we measured expression of caspase-1 in HUVECs using western blot analysis. The level of cleaved caspase-1 was upregulated with
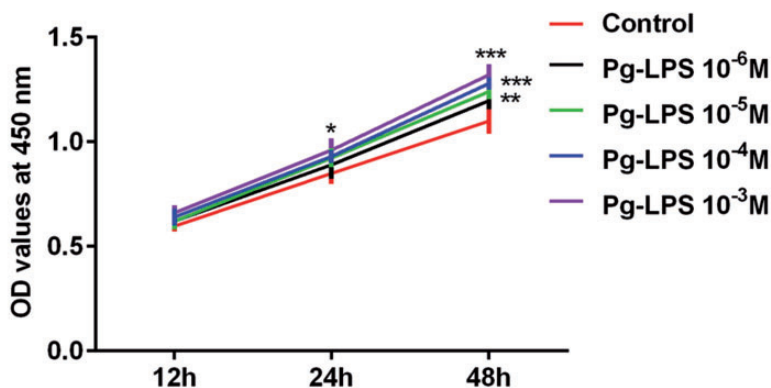
Figure 1. *Pg*-LPS promotes HUVEC proliferation, as measured by CCK-8 assay (and shown as optical density at 450 nm). *$P < 0.05$, **$P < 0.01$, ***$P < 0.001$; error bars represent standard deviation. *Pg*-LPS, *Porphyromonas gingivalis*-lipopolysaccharide; HUVECs, human umbilical vein endothelial cells; CCK-8, Cell Counting Kit–8.
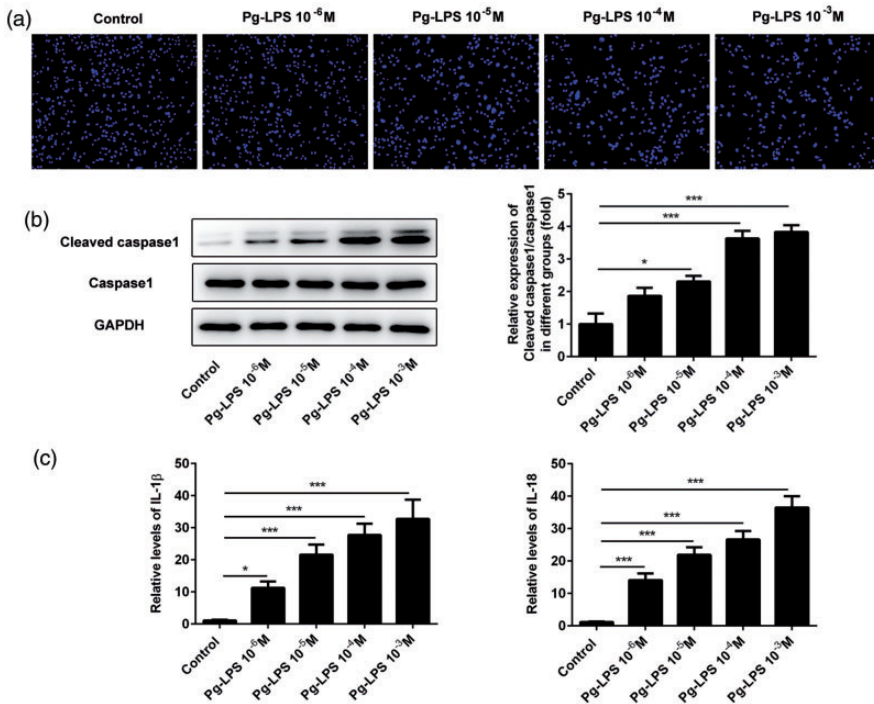
Figure 2. *Pg*-LPS promotes pyroptosis in HUVECs. (a) Representative photographs of DAPI-stained cells treated with *Pg*-LPS. (b) Images of immunoblotting for cleaved caspase-1, caspase-1, and GAPDH (loading control). (c) Secretion levels of IL-1β and IL-18 detected using ELISA. *$P < 0.05$, **$P < 0.01$, ***$P < 0.001$; error bars represent standard deviation.
*Pg*-LPS, *Porphyromonas gingivalis*-lipopolysaccharide; HUVECs, human umbilical vein endothelial cells; IL-1β, interleukin 1β; DAPI, 4′,6-diamidino-2-phenylindole.

increasing doses of *Pg*-LPS (Figure 2b). It has been reported that activation of caspase-1 induces secretion of IL-1β and IL-18 during pyroptosis.[23] Therefore, ELISA was used to detect the levels of IL-1β and IL-18 in the supernatants of cultured HUVECs. We found that expression of IL-1β and IL-18 was increased with increasing doses of *Pg*-LPS (Figure 2c).

circPPP1CC directly targeted and suppressed miR-103a-3p and miR-107 expression

To further explore the effect of circPPP1CC on pyroptosis, HUVECs were stably transfected with siRNA targeting circPPP1CC.

Overexpression plasmids of miR-103a-3p and miR-107 were constructed and transfected into HUVECs for subsequent experiments. The effects of plasmids used to silence circPPP1CC and overexpress miR-103a-3p and miR-107 were verified by reverse transcription (RT)-PCR. As shown in Figure 3a and Figure 3b, circPPP1CC was downregulated in knockdown groups, whereas miR-103a-3p and miR-107 were upregulated in mimic groups compared with the negative control (NC) groups. It is generally considered that circRNAs modulate the regulatory effects of miRNAs on their targeting proteins. Therefore, the Targetscan software (http://www.targets can.org/vert_72/) was used to predict the
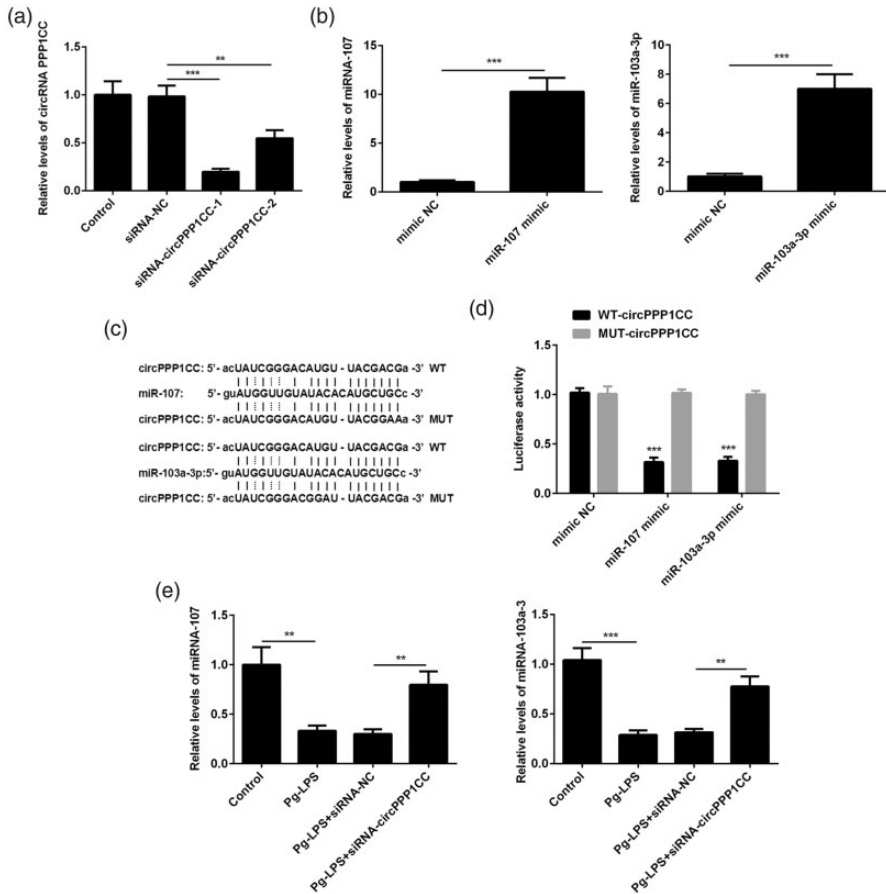
Figure 3. circPPP1CC targets miR-107 and miR-103a-3p and inhibits their expression. (a) Silencing of circPPP1CC with siRNA confirmed by RT-PCR. (b) Overexpression of miR-103a-3p and miR-107 with mimics detected using RT-PCR. (c) Predicted binding sites between circPPP1CC and miR-107 or miR-103a-3p. (d) Luciferase activity in NC, miR-107, and miR-103a-3p mimics groups. (e) Relative expression of miR-107 and miR-103a-3p in HUVECs, detected by RT-PCR following cell stimulation with *Pg*-LPS and transfection with siRNA targeting circPPP1CC. $*P < 0.05$, $**P < 0.01$, $***P < 0.001$; error bars represent standard deviation.

circPPP1CC, circular RNA serine/threonine-protein phosphatase PP1-gamma catalytic subunit; siRNA, short interfering RNA; NC, negative control; RT-PCR, reverse transcription PCR; HUVECs, human umbilical vein endothelial cells; *Pg*-LPS, *Porphyromonas gingivalis*-lipopolysaccharide.

miRNAs that were targeted by circPPP1CC. Bioinformatics analysis predicted that miR-103a-3p and miR-107 were directly targeted by circPPP1CC, whereas HMGB1, a pyroptosis-related protein, was a target protein for both miRNAs. The potential binding sites between circPPP1CC and miR-103a-3p and miR-107 are shown in Figure 3c. Therefore, luciferase assays were performed to identify the regulatory effects of circPPP1CC on miR-103a-3p and miR-107. Luciferase activity was decreased in HUVECs cotransfected with wild type (wt) or mutant (mut) circPPP1CC and miR-103a-3p or miR-107 mimics (Figure 3d). This finding

indicated that circPPP1CC directly targeted miR-103a-3p and miR-107. Furthermore, expression of miR-103a-3p and miR-107 was detected in the circPPP1CC knockdown and NC groups using RT-PCR. The results showed that stimulation with *Pg*-LPS (10^{-4} mol/L) downregulated miR-103a-3p and miR-107 expression compared with the control group (Figure 3e), whereas silencing of circPPP1CC rescued expression of both miRNAs.
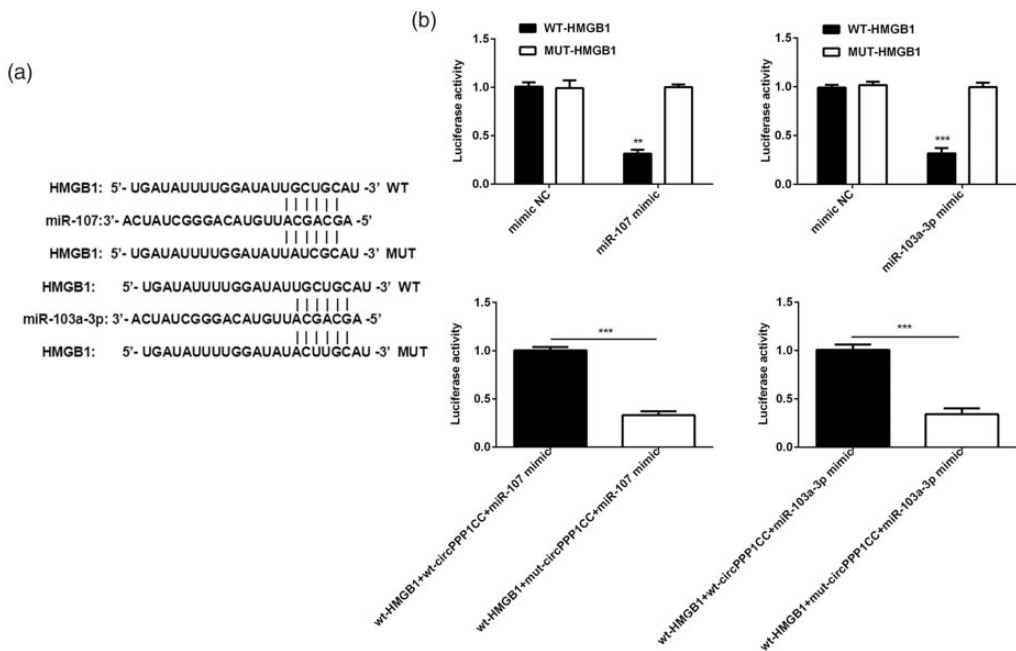
circPPP1CC attenuated the inhibitory effect of miR-103a-3p and miR-107 on HMGB1 expression

Subsequently, we explored the targeting efficacy of miR-103a-3p and miR-107 on *HMGB1* expression. The potential binding sites between *HMGB1* and miR-103a-3p or miR-107 are shown in Figure 4a. Luciferase assays were performed to reveal the associations between *HMGB1* and miR-103a-3p and miR-107. Luciferase activity was clearly reduced in the wt-HMGB1 and miR-103a-3p or miR-107 mimic reaction system (Figure 4b). However, activity was restored when wt-circPPP1CC was added into the reaction system.

Knockdown of circPPP1CC attenuated pyroptosis and inhibited HUVEC proliferation

The CCK-8 assay was conducted to detect changes in the proliferation of HUVECs following circPPP1CC knockdown. As shown in Figure 5a, stimulation of HUVECs with


Figure 4. circPPP1CC alleviated the inhibitory effect of miR-107 and miR-103a-3p on *HMGB1* expression. (a) Predicted binding sites between *HMGB1* and miR-107 or miR-103a-3p. (b) Luciferase activity determined between *HMGB1* and miR-107 or miR-103a-3p. **$P < 0.01$, ***$P < 0.001$; error bars represent standard deviation.
circPPP1CC, circular RNA serine/threonine-protein phosphatase PP1-gamma catalytic subunit; HMGB1, high mobility group box 1; NC, negative control; wt, wild type; mut, mutant.

Pg-LPS (10^{-4} mol/L) accelerated their proliferation. However, HUVEC proliferation was reduced following transfection with siRNA targeting circPPP1CC. Pyroptosis of HUVECs was detected by DAPI staining, and knockdown of circPPP1CC restored the morphological changes observed in *Pg*-LPS–stimulated HUVECs (Figure 5b). Results from ELISA demonstrated that the levels of IL-1β, IL-18, and HMGB1 were reduced
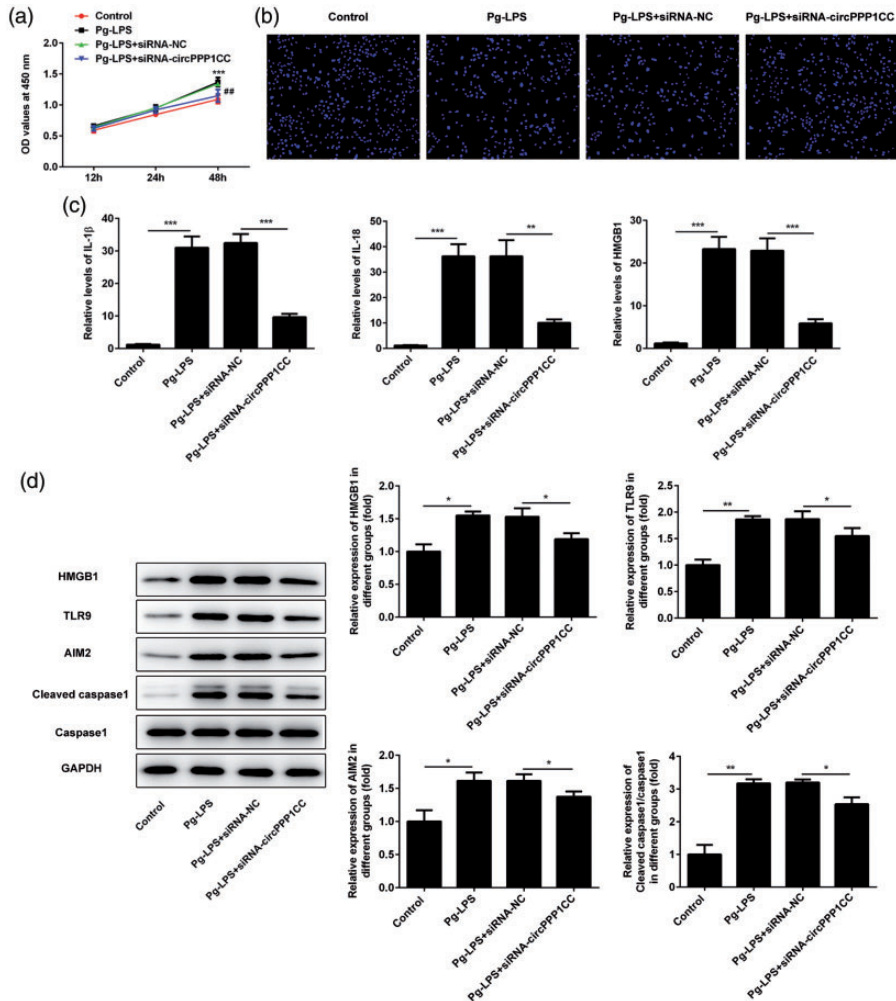

Figure 5. Knockdown of circPPP1CC restored pyroptosis in HUVECs. (a) Proliferation rate of HUVECs determined by CCK-8 assay following knockdown of circPPP1CC. (b) Pyroptosis in HUVECs detected by DAPI staining following knockdown of circPPP1CC. (c) Levels of proinflammatory cytokines IL-1β and IL-18 and HMGB1 detected using ELISA. (d) Images of immunoblotting for HMGB1, TLR9, AIM2, cleaved caspase-1, caspase-1, and GAPDH (loading control). *$P < 0.05$, **$P < 0.01$, ***$P < 0.001$; error bars represent standard deviation.
circPPP1CC, circular RNA serine/threonine-protein phosphatase PP1-gamma catalytic subunit; HUVECs, human umbilical vein endothelial cells; CCK-8, Cell Counting Kit-8; DAPI, 4′,6-diamidino-2-phenylindole; IL, interleukin; HMGB1, high mobility group box 1; TLR9, toll-like receptor 9; AIM2, absent in melanoma 2.

in cultured HUVEC supernatants in the circPPP1CC knockdown group (Figure 5c). The HMGB1/TLR9/AIM2 pathway is considered to induce pyroptosis; therefore, we detected levels of these proteins in HUVECs using western blot analysis. Results showed that expression of HMGB1, TLR9, and AIM2 was upregulated following cell stimulation with *Pg*-LPS (Figure 5d) but decreased in HUVECs treated with siRNA targeting circPPP1CC. Cleaved caspase-1 is a biomarker of pyroptosis, and thus we determined its expression in different groups. Following knockdown of circPPP1CC, expression of cleaved caspase-1 was also downregulated (Figure 5d). Finally, the putative molecular mechanism underlying the effects of circPPP1CC, miR-103a-3p and miR-107 on HMGB1 is shown in Figure 6.

Discussion

Atherosclerosis is a severe disease originating in the blood vessels.[24] During the occurrence and development of atherosclerosis, instability and detachment of the atherosclerotic plaque on the inner surface of blood vessels leads to more serious circulatory diseases, including thrombosis and coronary artery cell damage.[8,25,26] However, apoptosis of VSMCs can lead to instability and rupture of the atherosclerotic plaque.[27] Thus, VSMCs play a critical role in the development of atherosclerosis. Several studies have demonstrated that the apoptosis-related cleaved caspase-3 is not significantly altered, whereas pyroptosis-related cleaved caspase-1 is upregulated in impaired VSMCs.[28] These results suggest that pyroptosis is associated with the pathogenesis of atherosclerosis. Additionally, a study has shown that periodontitis is
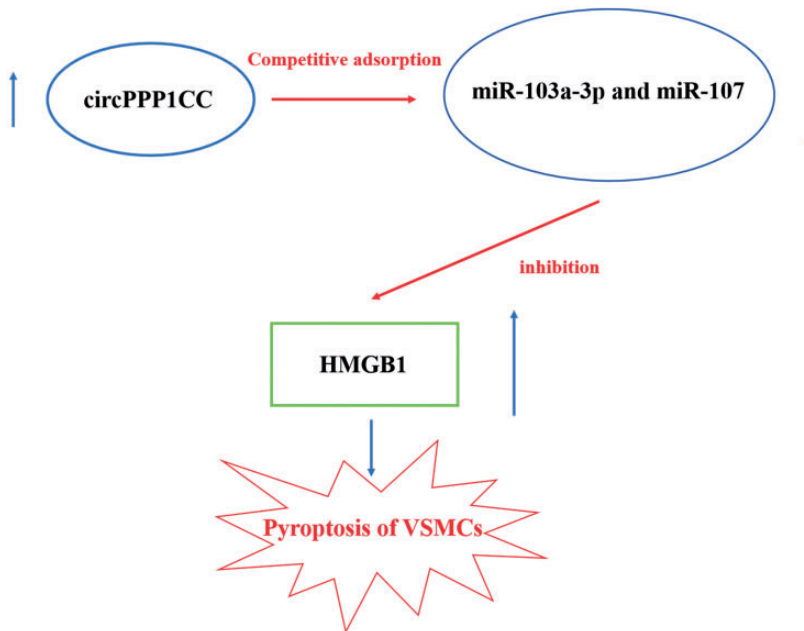
Figure 6. Diagram of the putative molecular mechanism underlying the effects of circPPP1CC, miR-103a-3p and miR-107 on HMGB1.
circPPP1CC, circular RNA serine/threonine-protein phosphatase PP1-gamma catalytic subunit; HMGB1, high mobility group box 1; VSMCs, vascular smooth muscle cells.

associated with atherosclerosis.[15] More specifically, it revealed that *Pg*-induced periodontitis promoted the development of atherosclerosis and that *Pg* was present in the atherosclerotic plaque.[14] Accumulating evidence suggests that *Pg* may induce the formation of amyloid plaques in brain tissues, leading to the occurrence of Alzheimer's disease.[29] The present study revealed that expression levels of cleaved caspase-1 and pyroptosis in VSMCs were increased following cell stimulation with *Pg*-LPS. Furthermore, secretion of IL-1β and IL-18 was increased in *Pg*-LPS–stimulated VSMCs. This finding was consistent with a previous report showing that activation of caspase-1 induced secretion of IL-1β and IL-18, resulting in cell inflammatory injury.[30] The aforementioned findings suggest that *Pg*-LPS may induce pyroptosis in VSMCs, thus promoting atherosclerosis and thrombosis.

Pyroptosis is an inflammatory type of programmed cell death that differs from apoptosis and necrosis. When acute injury is detected, AIM2 triggers the formation of the inflammasome, a protein complex, that participates in the induction of a cascade of inflammatory reactions, eventually leading to pyroptosis.[31] However, one study suggested that HMGB1 induced the formation of the inflammasome via TLR9/MyD88 pathway–mediated activation of AIM2.[32] CircRNAs, a type of non-coding RNAs, participate in and regulate several physiological processes.[33] It has been reported that circRNAs modulate the occurrence and development of atherosclerosis.[34] In the present study, Targetscan software was used to predict miRNAs targeting *HMGB1* and revealed that levels of miR-103a-3p and miR-107 were associated with HMGB1 and circPPP1CC. Furthermore, luciferase assays demonstrated that circPPP1CC acted as a "sponge" to competitively adsorb miR-103a-3p and miR-107, alleviating their inhibitory effect on expression of

HMGB1. In addition, *Pg*-LPS-induced pyroptosis and inflammatory response were relieved and expression of HMGB1, TLR9, AIM2, and cleaved caspase-1 was downregulated in VSMCs following knockdown of circPPP1CC. These results suggested that knockdown of circPPP1CC repressed adsorption of miR-103a-3p and miR-107. Therefore, upregulation of miR-103a-3p and miR-107 enhanced the inhibitory effect of circPPP1CC on the expression of *HMGB1*. The levels of *TLR9* and *AIM2* were also decreased following *HMGB1* downregulation, and pyroptosis of VSMCs was relieved. Taken together, these results indicated that inhibition of circPPP1CC could be applied to alleviate the symptoms of atherosclerosis and maintain the health of vascular tissues. However, we lack data from animal experiments to further confirm the effect of circPPP1CC on pyrolysis of VSMCs *in vivo* in this study. In subsequent experiments, we will verify the damaging effect of circPPP1CC on vascular smooth muscle through *in vivo* experiments in mice and further examine the expression of miR-103a-3p and miR-107 in these tissues.

Overall, results in the present study revealed that circPPP1CC could enhance *Pg*-LPS-induced pyroptosis of VSMCs by activating the HMGB1/TLR9/AIM2 pathway. Therefore, pyroptosis of VSMCs may promote the development of atherosclerosis, thus providing a novel target and potential therapy for the clinical treatment of atherosclerosis.

Availability of data

The analytical data in this study can be obtained from the corresponding author upon reasonable request.

Declaration of conflicting interest

The authors declare that there is no conflict of interest.

ORCID iD

Jijin Zhu (iD) https://orcid.org/0000-0002-9428-853X

References

1. Weber C and Noels H. Atherosclerosis: current pathogenesis and therapeutic options. *Nat Med* 2011; 17: 1410–1422.
2. Herrington W, Lacey B, Sherliker P, et al. Epidemiology of atherosclerosis and the potential to reduce the global burden of atherothrombotic disease. *Circ Res* 2016; 118: 535–546.
3. Chiong M, Morales P, Torres G, et al. Influence of glucose metabolism on vascular smooth muscle cell proliferation. *Vasa* 2013; 42: 8–16.
4. Johnson JL. Emerging regulators of vascular smooth muscle cell function in the development and progression of atherosclerosis. *Cardiovasc Res* 2014; 103: 452–460.
5. Li Y, Miao YS, Fu Y, et al. Attenuation of *Porphyromonas gingivalis* oral infection by α-amylase and pentamidine. *Mol Med Rep* 2015; 12: 2155–2160.
6. Zhang Y, Wang XC, Bao XF, et al. Effects of *Porphyromonas gingivalis* lipopolysaccharide on osteoblast-osteoclast bidirectional EphB4-EphrinB2 signaling. *Exp Ther Med* 2014; 7: 80–84.
7. Clarke MC, Figg N, Maguire JJ, et al. Apoptosis of vascular smooth muscle cells induces features of plaque vulnerability in atherosclerosis. *Nat Med* 2006; 12: 1075–1080.
8. Ping S, Li Y, Liu S, et al. Simultaneous increases in proliferation and apoptosis of vascular smooth muscle cells accelerate diabetic mouse venous atherosclerosis. *PLoS One* 2015; 10: e0141375.
9. Wang P, Xu TY, Guan YF, et al. Vascular smooth muscle cell apoptosis is an early trigger for hypothyroid atherosclerosis. *Cardiovasc Res* 2014; 102: 448–459.
10. Naghavi M, Libby P, Falk E, et al. From vulnerable plaque to vulnerable patient: a call for new definitions and risk assessment strategies: Part II. *Circulation* 2003; 108: 1772–1778.
11. Rossi ML, Marziliano N, Merlini PA, et al. Different quantitative apoptotic traits in coronary atherosclerotic plaques from patients with stable angina pectoris and acute coronary syndromes. *Circulation* 2004; 110: 1767–1773.
12. Van De Veerdonk FL, Netea MG, Dinarello CA, et al. Inflammasome activation and IL-1β and IL-18 processing during infection. *Trends Immunol* 2011; 32: 110–116.
13. Wu X, Zhang H, Qi W, et al. Nicotine promotes atherosclerosis via ROS-NLRP3-mediated endothelial cell pyroptosis. *Cell Death Dis* 2018; 9: 171.
14. Chhibber-Goel J, Singhal V, Bhowmik D, et al. Linkages between oral commensal bacteria and atherosclerotic plaques in coronary artery disease patients. *NPJ Biofilms Microbiomes* 2016; 2: 7.
15. Suh JS, Kim S, Boström KI, et al. Periodontitis-induced systemic inflammation exacerbates atherosclerosis partly via endothelial-mesenchymal transition in mice. *Int J Oral Sci* 2019; 11: 21.
16. Ge X, Li W, Huang S, et al. The pathological role of NLRs and AIM2 inflammasome-mediated pyroptosis in damaged blood-brain barrier after traumatic brain injury. *Brain Res* 2018; 1697: 10–20.
17. Csak T, Pillai A, Ganz M, et al. Both bone marrow-derived and non-bone marrow-derived cells contribute to AIM2 and NLRP3 inflammasome activation in a MyD88-dependent manner in dietary steatohepatitis. *Liver Int* 2014; 34: 1402–1413.
18. Li X, Yang L and Chen LL. The biogenesis, functions, and challenges of circular RNAs. *Mol Cell* 2018; 71: 428–442.
19. Li HM, Ma XL and Li HG. Intriguing circles: Conflicts and controversies in circular RNA research. *Wiley Interdiscip Rev RNA* 2019; 10: e1538.
20. Wilusz JE. A 360° view of circular RNAs: From biogenesis to functions. *Wiley Interdiscip Rev RNA* 2018; 9: e1478.

21. Liu G, Deng J, Zhang Q, et al. *Porphyromonas gingivalis* lipopolysaccharide stimulation of vascular smooth muscle cells activates proliferation and calcification. *J Periodontol* 2016; 87: 828–836.

22. Hirasawa M and Kurita-Ochiai T. *Porphyromonas gingivalis* induces apoptosis and autophagy via ER stress in human umbilical vein endothelial cells. *Mediators Inflamm* 2018; 2018: 1967506.

23. Delaleu N and Bickel M. Interleukin-1 beta and interleukin-18: regulation and activity in local inflammation. *Periodontol 2000* 2004; 35: 42–52.

24. Menzyanova NG, Pyatina S, Nikolaeva ED, et al. Screening of biopolymeric materials for cardiovascular surgery toxicity: evaluation of their surface relief with assessment of morphological aspects of monocyte/macrophage polarization in atherosclerosis patients. *Toxicol Rep* 2019; 6: 74–90.

25. Falk E, Nakano M, Bentzon JF, et al. Update on acute coronary syndromes: the pathologists' view. *Eur Heart J* 2013; 34: 719–728.

26. Saffitz JE and Schwartz CJ. Coronary atherosclerosis and thrombosis underlying acute myocardial infarction. *Cardiol Clin* 1987; 5: 21–30.

27. Nahapetyan H, Moulis M, Grousset E, et al. Altered mitochondrial quality control in Atg7-deficient VSMCs promotes enhanced apoptosis and is linked to unstable atherosclerotic plaque phenotype. *Cell Death Dis* 2019; 10: 119.

28. Burzynski LC, Humphry M, Bennett MR, et al. Interleukin-1α activity in necrotic endothelial cells is controlled by caspase-1 cleavage of interleukin-1 receptor-2: implications for allograft rejection. *J Biol Chem* 2015; 290: 25188–25196.

29. Dominy SS, Lynch C, Ermini F, et al. *Porphyromonas gingivalis* in Alzheimer's disease brains: evidence for disease causation and treatment with small-molecule inhibitors. *Sci Adv* 2019; 5: eaau3333.

30. Wang J, Sahoo M, Lantier L, et al. Caspase-11-dependent pyroptosis of lung epithelial cells protects from melioidosis while caspase-1 mediates macrophage pyroptosis and production of IL-18. *PLoS Pathog* 2018; 14: e1007105.

31. Man SM, Karki R and Kanneganti TD. AIM2 inflammasome in infection, cancer, and autoimmunity: role in DNA sensing, inflammation, and innate immunity. *Eur J Immunol* 2016; 46: 269–280.

32. Wang J, Li R, Peng Z, et al. HMGB1 participates in LPS-induced acute lung injury by activating the AIM2 inflammasome in macrophages and inducing polarization of M1 macrophages via TLR2, TLR4, and RAGE/NF‑κB signaling pathways. *Int J Mol Med* 2020; 45: 61–80.

33. Chen LL and Yang L. Regulation of circRNA biogenesis. *RNA Biol* 2015; 12: 381–388.

34. Holdt LM, Stahringer A, Sass K, et al. Circular non-coding RNA ANRIL modulates ribosomal RNA maturation and atherosclerosis in humans. *Nat Commun* 2016; 7: 12429.